BeBeC-2016-D8

EXTENDED VERSION: IMPROVING THE DAMAS 2 RESULTS FOR WAVENUMBER-SPACE BEAMFORMING

Stefan Haxter
German Aerospace Center (DLR)
Bunsenstr. 10, 37073 Göttingen, Germany

Abstract

When using deconvolution algorithms for the improvement of beamforming results, the family of DAMAS-algorithms has shown to be very useful. One member of this family – the DAMAS 2 algorithm – comes into focus when one is concerned with computational speed and efficient memory usage. The algorithm is especially suited for wavenumber beamforming, since it expects a shift-invariant point-spread function for best results. During application of this method on wavenumber-beamforming, it was noticed that the results can be even improved when increasing the size of the point-spread function. This further enhancement of the algorithm will be presented in examples and discussed. The algorithm is compared to other deconvolution procedures by first applying it to synthetic data and comparing the algorithm output to the known solution. Afterwards the algorithm will be applied to experimental wind tunnel data and compared to the result from other deconvolution procedures as well. Given a shift-invariant point-spread function, the algorithm performs very well in terms of detailedness of the algorithm output at a moderate increase of computational effort.

1 INTRODUCTION

Ever since beamforming was introduced as an acoustic measurement technique, people have been trying to improve the results. This paper focuses on such an improvement technique.

The bare output of a beamformer is also called “dirty map”. The term “dirty” is used, since this direct output still contains signal processing artifacts dependent on the choice of steering vectors used. The influence of steering vector choice has been investigated by Sarradj [7] who found different peak positions and amplitudes when using different approaches for the microphone weighting. The influence of microphone distribution is reflected in the “point-spread function” (*PSF*), which resembles the beamformer output for a single unity source. This *PSF*

has two effects on the source display: firstly, it broadens the main lobe width of the peak from infinitely small to a finite value. Secondly, it introduces a limit to the dynamic range of the array by means of sidelobes. As the beamforming result are affected by the unwanted influence of the *PSF*, the question arises what the sources in the map look like without the influence of the *PSF*.

Mathematically, the dirty map is a convolution of the underlying source map (this is what one is interested in) and the *PSF*. With this in mind, as the dirty map is a convolution of the source distribution with the *PSF*, the source distribution can be obtained from the dirty map via deconvolution, if the *PSF* is known. Fortunately, if the Green's Function is known, the *PSF* can be calculated. If the Green's function is estimated, the *PSF* will be an estimate as well, but it will be still a reasonable estimate.

In the acoustic community, several algorithms have been published in order to approach the deconvolution problem. In this paper, two of them are addressed: DAMAS (a *D*econvolution *A*pproach for the *M*apping of *A*coustic *S*ources) by Thomas Brooks [2] can deal with shift-variant *PSF*s and does so by mapping the influence of each steering grid point to any to any other point in the map. Due to the - oftentimes - large amount of steering grid points the algorithm requires a lot of both, computation time and memory. Another algorithm, DAMAS 2, was introduced by Robert Dougherty as an extension of DAMAS [3]. DAMAS 2 performs considerably better than DAMAS in terms of speed and memory usage. However it expects *PSF*s that are shift-invariant and is therefore limited to array measurements where the source region is small compared to the distance between array and source region. DAMAS 2 is very suitable for measurements where the sources are infinitely far away from the array [3], such as wavenumber beamforming [5], since the *PSF*s in such a case are shift-invariant. Due to its computational efficiency, DAMAS 2 has shown to be a good tool for the analysis of wavenumber maps [6].

In contrast to mapping the influence of each point in the steering map to any other point in the steering map, the DAMAS 2 algorithm is limited to the influence of only one point to all other points. This can lead to a limitation in the quality of the deconvolution process. In former versions of the algorithm, a regularization filter was introduced in order to overcome the effect of high-frequency[1] noise. The filter acts as a low-pass filter of the *PSF* which then sets a limit to the resolution of the algorithm output. In the current paper, an enhancement of the DAMAS 2 algorithm is shown, which will eliminate this particular limitation and makes the usage of the low-pass filtering obsolete. This enhancement has been mentioned by Bahr [1], but it has not been compared to the other implementations of DAMAS 2 or applied to wavenumber spectra obtained experimentally.

The paper is structured as follows: first, the functionality of the DAMAS 2-algorithm is described and the point of enhancement is identified. Then, the implementation of the enhancement is shown and tested with synthetic data. The synthetic data will be convolved with the *PSF* and the algorithms are then applied to again obtain the synthetic data. After presenting the synthetic data analysis, the algorithms are applied to wavenumber spectra created from experimental data.

[1] The usage of the term "frequency" as "cycles per second" here is a representative of any unit that is present after the Fourier transform

2 THE DAMAS 2 ALGORITHM

The DAMAS 2-algorithm performs the convolution of source distribution and PSF entirely in the frequency domain. This is why it works very efficiently in terms of computation time and memory usage. The computation can be divided into the following steps (taken from reference [3]; applied to wavenumber space). i is the iteration index:

1. Compute $PSF\left(\vec{x}\right) = FFT\left(psf\left(\vec{k}\right)\right)$
2. Set $a = \sum_{k_x,k_y} |psf|$
3. Set solution $q^1\left(\vec{k}\right) = 0$ for each $\vec{k}$ in the beamforming grid.
4. Iterate
   a) $Q\left(\vec{x}\right) = FFT\left(q^i\left(\vec{k}\right)\right)$
   b) For each $\vec{k}$, scale $Q\left(\vec{x}\right)$ by $\exp\left(-\vec{x}^2/\left(2\vec{x}_c^2\right)\right)$
   c) Let $R\left(\vec{x}\right) = PSF\left(\vec{x}\right) \cdot Q\left(\vec{x}\right)$ for each $\vec{x}$
   d) $r\left(\vec{k}\right) = FFT^{-1}\left(R\left(\vec{x}\right)\right)$
   e) $q^{i+1}\left(\vec{k}\right) = q^i\left(\vec{k}\right) + \left|b\left(\vec{k}\right) - r\left(\vec{k}\right)\right|/a$ for each $\vec{k}$.
   f) Replace each negative value of $q^{i+1}\left(\vec{k}\right)$ by 0

In step 4.c. the PSF is convolved with the source map Q via multiplication in the "frequency"-domain. The size $[n_x, n_y]$ of the PSF is the same as the source map:

$$n_{x,PSF} = n_{x,Q} \tag{1}$$

$$n_{y,PSF} = n_{y,Q} \tag{2}$$

The position of the peak in the PSF can be chosen arbitrarily. If the position of the peak is chosen in the center, the PSF has equal influence towards all directions. The filter step 4.b. is required to suppress high-frequency noise that occurs in the data. The cutoff position of the filter is resembled by the factor x_c. Note that the original implementation of DAMAS 2 was focused on regular beamforming maps in the spatial domain ($q = q(\vec{x})$), which lead to the wavenumber space after applying the Fourier transform ($Q = Q(\vec{k})$). The present investigation displays the resulting maps in the wavenumber space ($q = q(\vec{k})$). Therefore, the Fourier transformed maps are located in the spatial domain ($Q = Q(\vec{x})$).

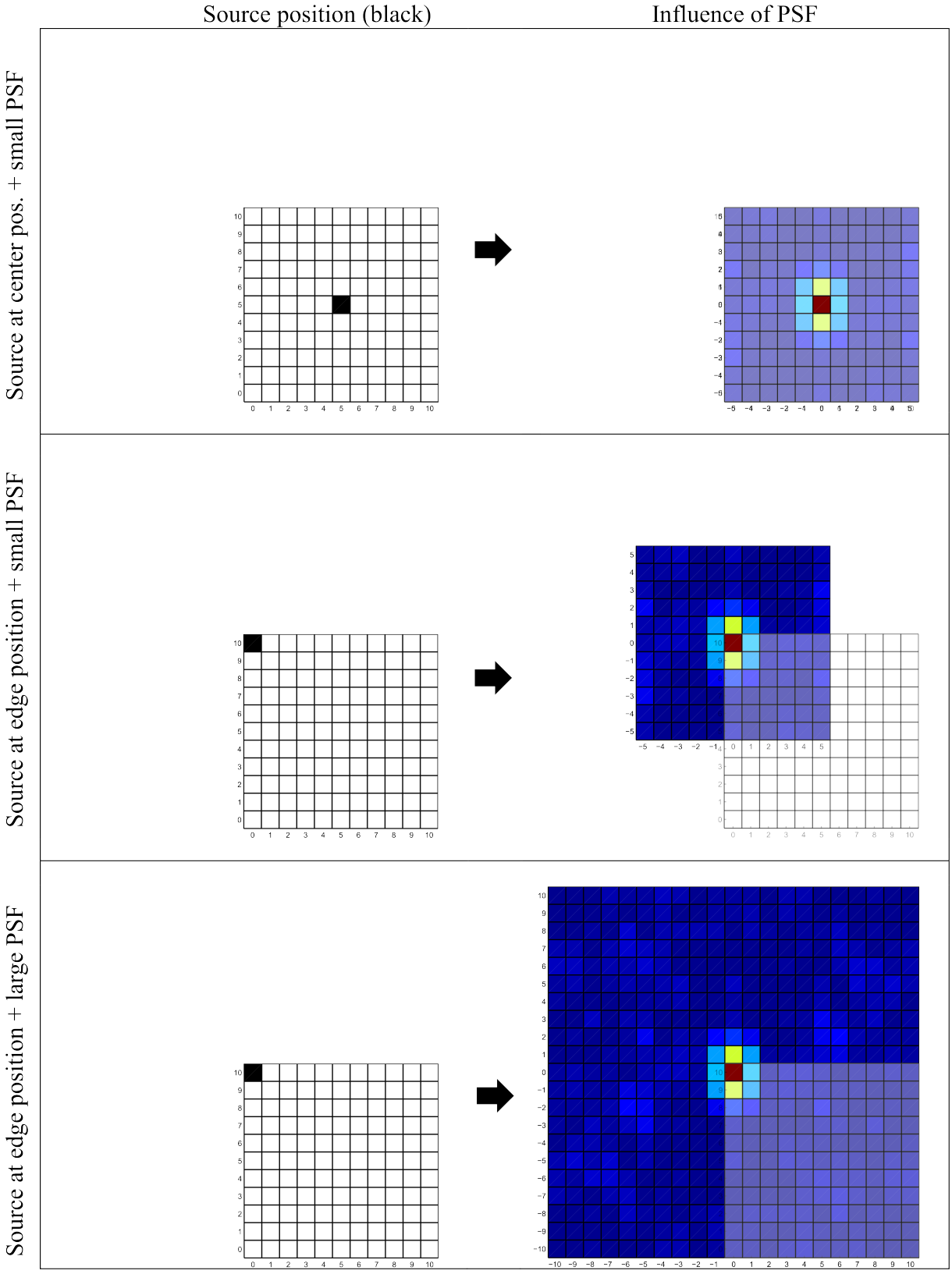

Figure 1: Influence of differently-sized PSFs on the dirty map.

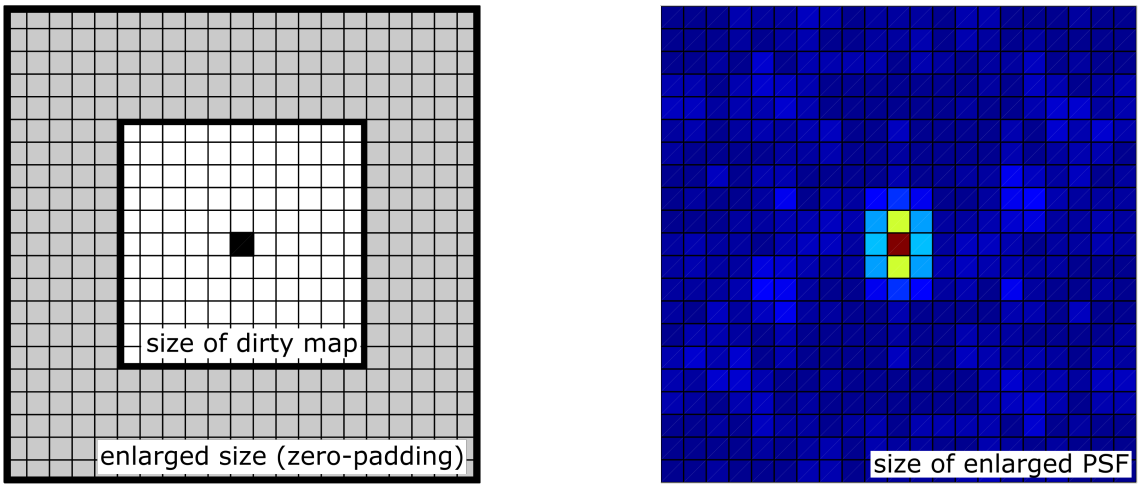

Figure 2: Illustration of how the dirty map is zero-padded.

3 EXTENDING THE PSF - DAMAS 2.1

The influence of the point spread function on the points in the dirty map is shown in figure 1. If dirty map, source map, and *PSF* all have the same size, a source located in the very center of the map will affect all the points on the grid. As the source position is moved away from the center of the map (shown in the middle), the PSF does not affect all the points any more (shown by the blank fields). This can lead to considerable deviation when iterating for the underlying source map as will be shown later. Implementing a larger *PSF* with sizes

$$\hat{n}_{x,PSF} = 2 \cdot n_{x,Q} - 1 \tag{3}$$

$$\hat{n}_{y,PSF} = 2 \cdot n_{y,Q} - 1 \tag{4}$$

can improve the result. The implementation of this in the code can be accomplished by zero-padding the dirty map b in all directions as illustrated in figure 2.

$$\hat{b} = \begin{cases} 0 & \forall\,(\hat{n}_x < n_x/2+1) \vee (\hat{n}_y < n_y/2+1) \\ 0 & \forall\,(\hat{n}_x > 3n_x/2+1) \vee (\hat{n}_y < 3n_y/2+1) \\ b & else \end{cases} \tag{5}$$

The algorithm leads to an enlarged reconstructed dirty map $\hat{r}$. For the calculation of a residual only the center part of the reconstructed map and the dirty map is compared.

4 TEST CASE 1: SYNTHETIC DATA

A test case was set up, comparing the results of several different deconvolution algorithms to the original image. The test case image is shown in figure 3 (a) and has the following features:

- Distributed sources rather than point sources

- Various different source levels (the amplitude of the structure is rising linearly from 0 on the left to 1 on the right; corresponding to $-\infty dB$ to $0\,dB$)
- Sources at the edge of the map
- Different separated source regions. The will be referred to as the "text part" and the "signet part"

Algorithm	N	k_c [m^{-1}]	Execution time [s]		
			100 Hz	1000 Hz	2500 Hz
DAMAS 2	10^1	$\pi/(2\Delta k)$	0.062	0.060	0.023
DAMAS 2	10^5	$\pi/(2\Delta k)$	165	156	178
DAMAS 2 - no regularization	10^1	none	0.021	0.019	0.016
DAMAS 2 - no regularization	10^5	none	153	164	182
DAMAS 2.1 (enlarged)	10^1	none	0.032	0.077	0.033
DAMAS 2.1 (enlarged)	10^5	none	397	293	330
DAMAS	10^1	none	22	22	23
DAMAS	10^5	none	1.25×10^5	1.25×10^5	1.42×10^5

Table 1: Summary of the deconvolution parameters

The number of points in the image was $n_x = 89$ points in k_x-direction and $n_y = 77$ points in k_y-direction, leading to a total number of $M = 6853$ points. The limits of the normalized axes were for $k_x : \pm 10k_0$ and for $k_y : \pm 8.24k_0$. $k_0(f)$ is the wavenumber of pressure fluctuations propagating at the speed of sound. The normalization of all wavenumber maps with this frequency-dependent value is a very reasonable implementation: firstly, the dependency of the map size on frequency is eliminated, and secondly, effects caused by acoustic propagation become easily identifiable. Synthetic data at three different frequencies were used and the number of iterations was varied in order to estimate the performance each algorithm. An array distribution of 48 microphones was used to set up the synthetic data. The distribution is shown in figure 4 and it is the same transducer distribution that was used in the experimental test case.

The corresponding *PSF* of the microphone distribution at a frequency of $f = 1\,\text{kHz}$ for a point source at $k_x = k_y = 0\,\text{m}^{-1}$ is shown in figure 3 (b). The whole *PSF* as it would affect a beamforming result is depicted in that figure. The originally-used small *PSF* (which has the same size as the dirty map) is limited to within the black rectangle in figure 3 (b). The different effect of this is seen when the source map is convolved with each of the two *PSF*s of different size. In figure 2(c), the convolution of the source map with the large *PSF* is shown. The large extend of the *PSF* leads to an even distribution of background noise. When the outer part of the *PSF* is neglected (equivalent of setting all values of the PSF outside the rectangle to zero), the dirty map has a larger amplitude variation and an uneven background noise level. (shown in figure 3 (e)). The maximum in the map stays approximately the same. In order to tell, which dirty map is more appropriate, a cross-correlation matrix was generated from the source map and a the dirty map from regular beamforming, C, was obtained and subtracted from the convolution results. This is shown for both, the small and the large *PSF* in figures 3 (e) and 3 (d). While the result from the large *PSF* approximates the beamforming results very well,

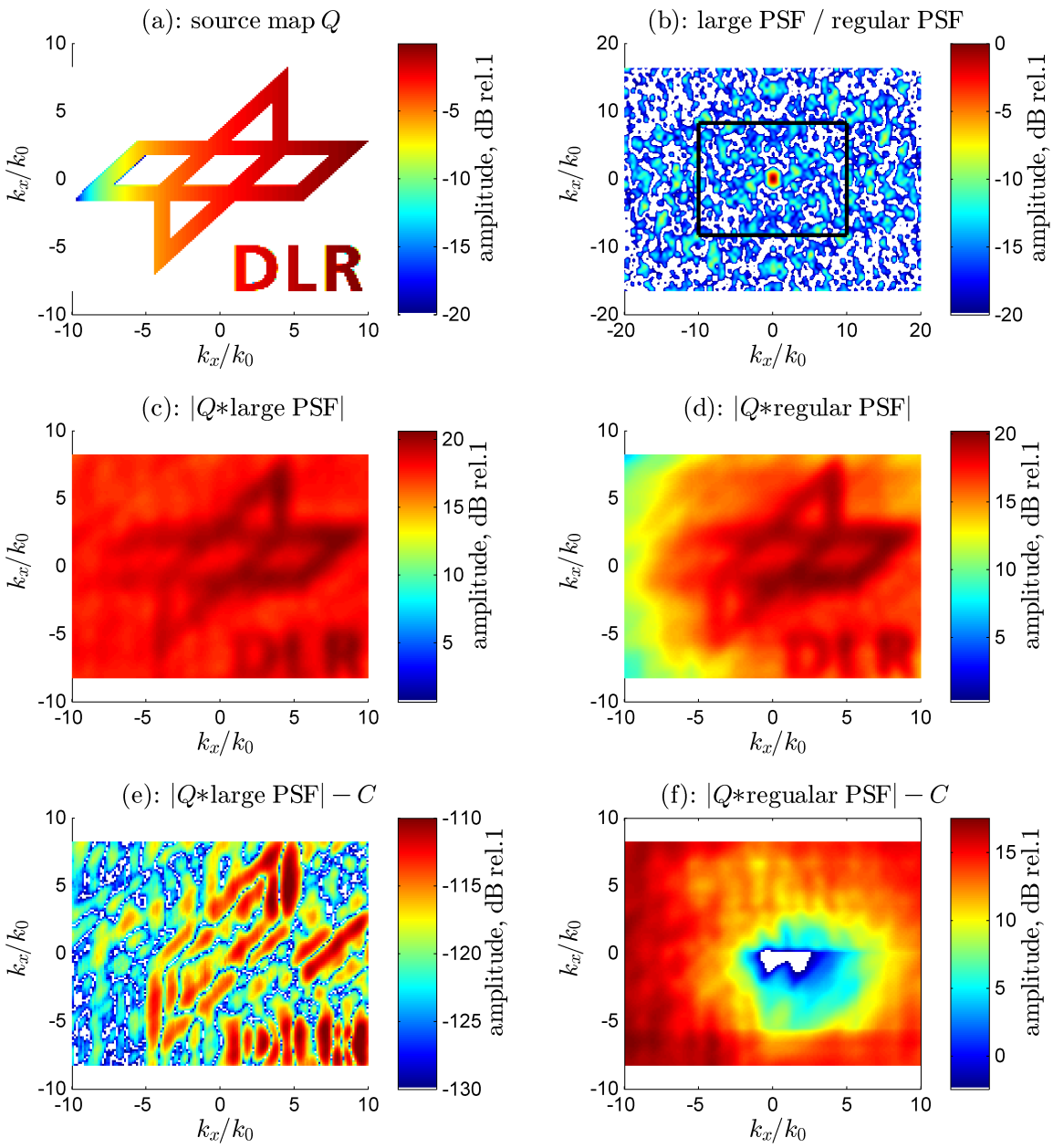

Figure 3: (a) source distribution of the synthetic test case
(b) whole figure: large PSF; area in the rectangle: small PSF at 1 kHz
(c) convolution of source map with large PSF at 1 kHz
(d) convolution of source map with small PSF at 1 kHz
(e) difference between convolution of source map with large PSF and beamforming result
(f) difference between convolution of source map with small PSF and beamforming result

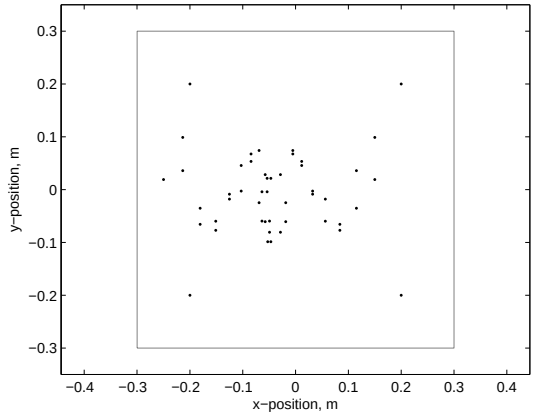

Figure 4: Transducer distribution for the setup of synthetical data and transducer distribution in the subsequent experimental data analysis

the result using the small *PSF* differs strongly from the beamforming result. The dirty map from convolving the source map with the large *PSF* is therefore seen as the one to use in the reconstruction process of the DAMAS 2 algorithm. Note that the good approximation of the result via convolution only applies to cases where the *PSF* is shift-invariant. A regularization parameter x_c for the Gaussian low-pass filter was used for one of the comparative cases with regular DAMAS 2 deconvolution. Similar to Ehrenfried&Koop [4] the parameter x_c was chosen to be

$$x_c = 0.5\pi/\Delta k_c. \tag{6}$$

No regularization filter was applied when using the large *PSF*. The execution time was measured using the tic and toc command in Matlab on a PC with an Intel Xeon CPU E5-2650 @ 2.00Ghz and 40GiB of RAM. The times presented were obtained while calculating three maps in parallel on the same machine. They are therefore rough estimates and are used only to show the order of magnitude of the computation time required.

5 RESULTS FROM SYNTHETIC DATA

Three different frequencies were chosen for testing the algorithms: 100 Hz, 1000 Hz, and 2500 Hz. The effect of each different frequency is the different scaling between source map and *PSF*.

5.1 100 Hz

For the case under consideration, a low frequency yields a *PSF* which is dominated by the main lobe. The effect of this can be seen in figure 5 (b) where the dirty map for this case is displayed. Due to the large main lobe width, the combination of the distributed sources causes a large rise in amplitude up to approximately 25 dB. The shape of the dirty map appears as a large ”blob” - an undefined structure which does not even roughly allows to determine the underlying shape shown in figure 5 (a). After $N = 10^1$ iterations, the three variations of the

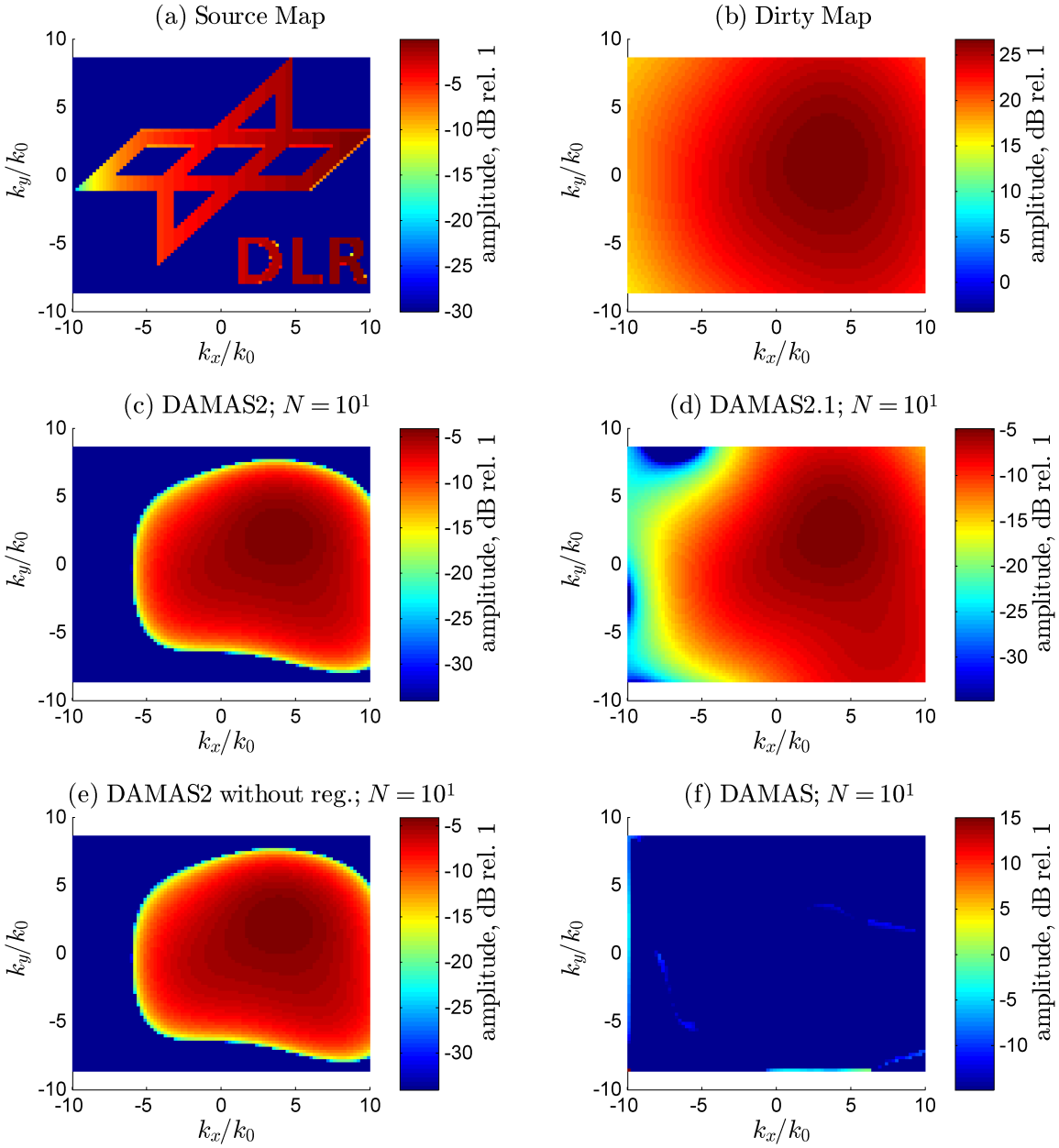

Figure 5: Results for a frequency of $f = 100\,\mathrm{Hz}$ after $N = 10$ iterations
(a) source distribution of the synthetic test case
(b) dirty map
(c) result from DAMAS 2 with regularization filter
(d) result from DAMAS 2.1
(e) result from DAMAS 2 without regularization filter
(f) result from DAMAS

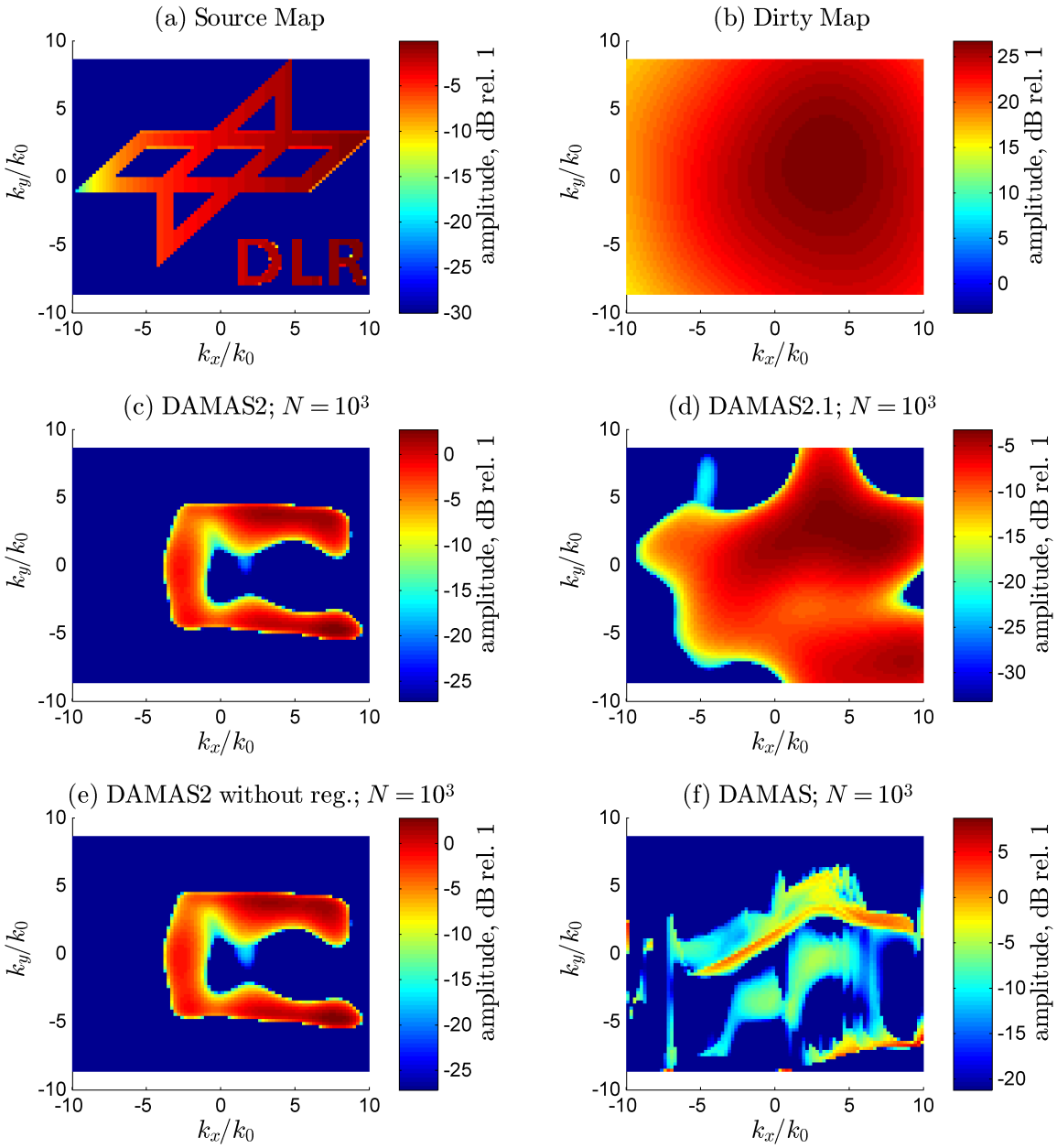

Figure 6: Results for a frequency of $f = 100\,\mathrm{Hz}$ after $N = 1000$ iterations
(a) source distribution of the synthetic test case
(b) dirty map
(c) result from DAMAS 2 with regularization filter
(d) result from DAMAS 2.1
(e) result from DAMAS 2 without regularization filter
(f) result from DAMAS

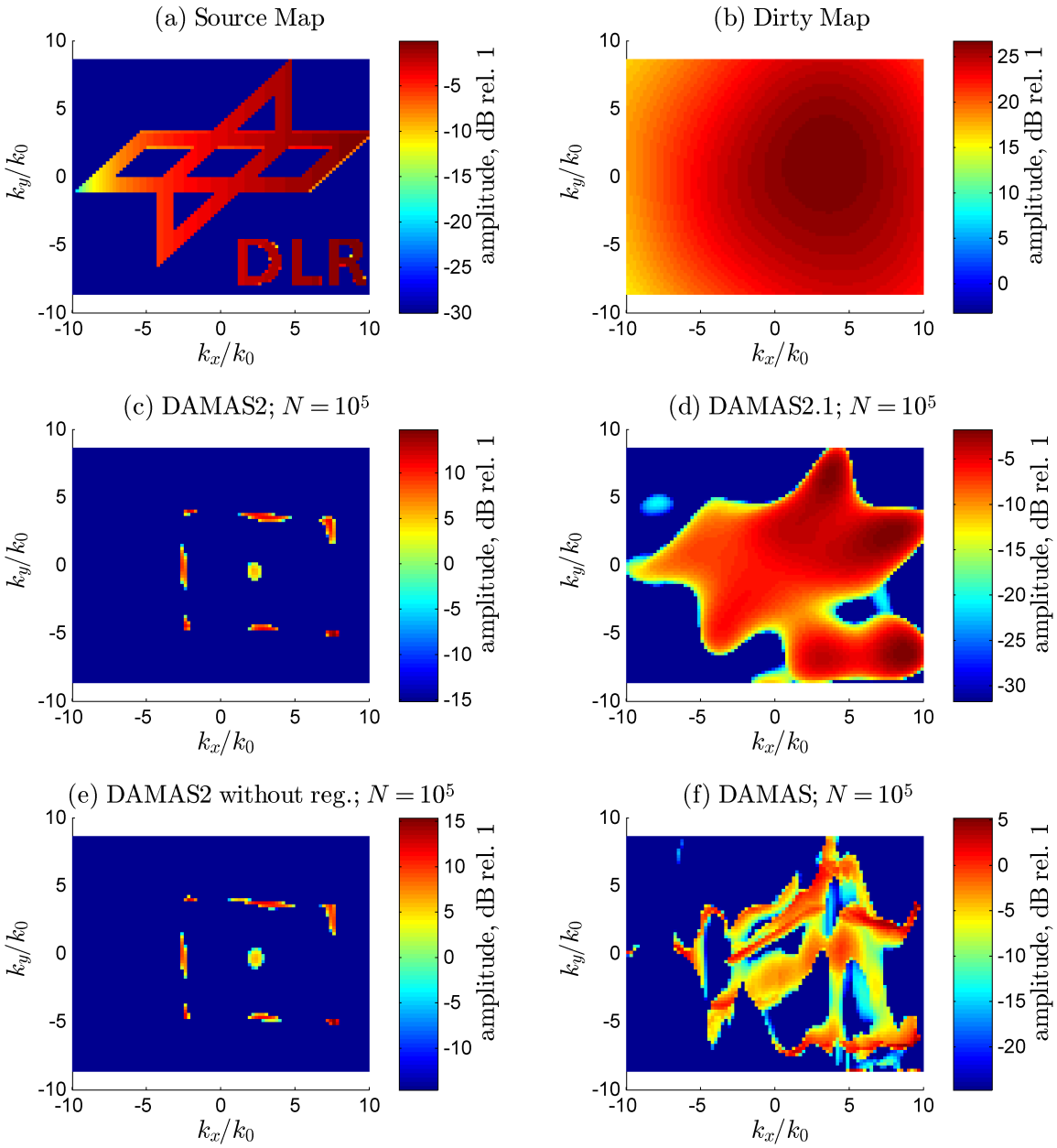

Figure 7: Results for a frequency of $f = 100\,\mathrm{Hz}$ after $N = 100000$ iterations
(a) source distribution of the synthetic test case
(b) dirty map
(c) result from DAMAS 2 with regularization filter
(d) result from DAMAS 2.1
(e) result from DAMAS 2 without regularization filter
(f) result from DAMAS

DAMAS 2-algorithms have reduced the amplitude of the dirty map to a reasonable level, but did not change the shape or yielded any more detail about the shape of the source map. The difference between the result from the DAMAS 2-algorithm with regularization filter and the result from the DAMAS 2 algorithm without regularization filter is minimal, since the *PSF* already is dominated by small "frequencies"[2] which are not affected by the regularization filter. The DAMAS-algorithm was able to reduce the amplitude over the major part of the map too. The maximum of the colorbar - which is set to the maximum in the map - shows that some peak values are present which are very dominant.

Results for a frequency of $f = 100\,\text{Hz}$ after $N = 10^3$ iterations are shown in figure 6. The amplitude of the results DAMAS 2 and DAMAS 2 without regularization algorithms has increased by approximately 5 dB and is now clearly above the level of the source map. The shape has changed to a "C"-shaped structure which appears more detailed than a blob, but is very different from the source map. The DAMAS 2.1 algorithm has maintained its amplitude level which is still comparable to the source map amplitude. The basic shape of the structure is already recognizable and the amplitude variation from left to right is indicated. The DAMAS-algorithm has suggested a source map which consists of few dominant lines with intermediate areas of sources. Several dominant parts of the map - like the dominant lines in the center and the presence of sources in the lower right "text-part" corner are located at approximately the right place. Especially on the left side of the source map, several dominant spikes are present.

When increasing the number of iterations even further to $N = 10^5$ iterations (figure 7), the characterizations already seen at $N = 10^3$ iterations become even more distinct: The "C"-shaped structure resulting from the DAMAS 2 algorithm with and without regularization exhibits sharp edges and has produced a center source. The amplitude has increased even further. The DAMAS 2.1 algorithm has produced a clear image of the basic structure at reliable amplitude. Even the split between the text part of the source map and the signet part of the source map is distinguishable. The result from the DAMAS algorithm has further proceeded towards a map with line-like source structures in the signet-part of the map. The lines are roughly located in the right area, but no distinct shape can be recognized. The amplitude of these structures is slightly increased in comparison with the original source map.

5.2 1000 Hz

The dirty map resulting from convolving the source map with a *PSF* generated for a frequency of $f = 1000\,\text{Hz}$ is shown in figure 8. Some source map features such as shape of the text part and the signet part are already recognizable from the dirty map. The amplitude of the whole map is however increased and a lot of background noise is present due to the side lobes of the *PSF*. After $N = 10$ iterations, the basic shape of the source map is preserved by all the algorithms. The DAMAS 2 algorithm with regularization has reduced the amplitude to a level slightly above the level of the source map (figure 8 (c)). Still there is excessive background noise present. The DAMAS 2.1 algorithm has reduced the amplitude even further to a plausible amount. The contrast of the result is however still very low. The DAMAS 2-algorithm without regularization filter was able to reduce the amplitude to a plausible amount and increase the contrast between sources and background. There is now a difference between the results from

[2]The usage of the term "frequency" as "cycles per second" here is a representative of any unit that is present after the Fourier transform of the dirty map

the regular DAMAS 2 algorithm and the DAMAS 2-algorithm without regularization since the *PSF* is not dominated by low-"frequency" elements anymore and the regularization considerably changes the *PSF* used for reconstruction. The result from the DAMAS-algorithm exhibits a number of point-like source which already strongly hint towards the underlying signet source structure. The background level has been reduced to a very low level and the sources clearly stand out. On the left side of the map, a very dominant line structure, which is not present in the original source map, is yet present.

After $N = 10^3$ iterations, the amplitude of the result from the regular DAMAS 2 algorithm has increased again to a level close to the level of the dirty map (figure 9 (c)). The contrast of the image is however increased as well. The result of the DAMAS 2.1 algorithm resembles a very close approximation of the original source map (figure 9 (d)). Both, amplitude and shape are reconstructed very well and all characteristics of the source map are recognizable. The DAMAS 2 algorithm without regularization yields a reasonable representation of the shape and amplitude as well (figure 9 (e)). However, the result appears perforated with larger holes where the source map has low amplitude and with less holes where the amplitude of the source map is higher. It seems like the algorithm is trying to assemble the source map from spikes rather than from distributed sources. The distributed character of the sources is not reconstructed well. The result from the DAMAS-algorithm in figure 9 (f) shows a shape that is very well recognizable as the signet structure of the original source map. As for the DAMAS 2 algorithm without a regularization filter, the resutl from the DAMAS-algorithm appears to be made up from spikes rather than a continuous surface. The dominant ones of these spikes have a source level that is too high. The background noise and side lobes are suppressed very well.

Increasing the number of iterations to $N = 10^6$ yields the results shown in figure 10. Both, the results from the DAMAS 2 algorithm and the DAMAS 2 algorithm without regularization have produced a map consisting of spikes with high amplitude. The algorithm using a filter yields a result with few high-amplitude broad spikes which even top the amplitude in the dirty map by 10 dB. The algorithm without regularization exhibits many narrow spikes which are aligned in the basic shape of the underlying source map. The amplitude of the many narrow spikes lies approximately 15 dB above the original level of the source map. The difference between the maps reconstructed with and without regularization filter can be once again explained by the filtering out of high "frequency" content from the *PSF* which is not available for reconstruction after filtering. Both algorithms cannot deal with distributed sources and will display them as a distribution of spikes. Like after $N = 10^3$ iterations, the DAMAS 2.1 algorithm has produced a map that comes very close to the original image. The edges of the signet structure and the text now appear even a little more sharpened. The result from the DAMAS algorithm change only little with further increasing the number of iterations. The signet structure of the original source map is clearly visible and the spikedness of the source distribution has flattened out slightly compared to the case after $N = 10^3$ iterations. The amplitudes of the dominant spikes is however still too high.

5.3 2500 Hz

At a high frequency of $f = 2500$ Hz, the amplitude of the dirty map for this case only increases to approximately 20 dB above the level of the source map. The reason for this is the relatively narrow main lobe width at this frequency which reduces the effect of amplitude increment due to distributed sources. The dominant effect visible in the dirty map is the increased background

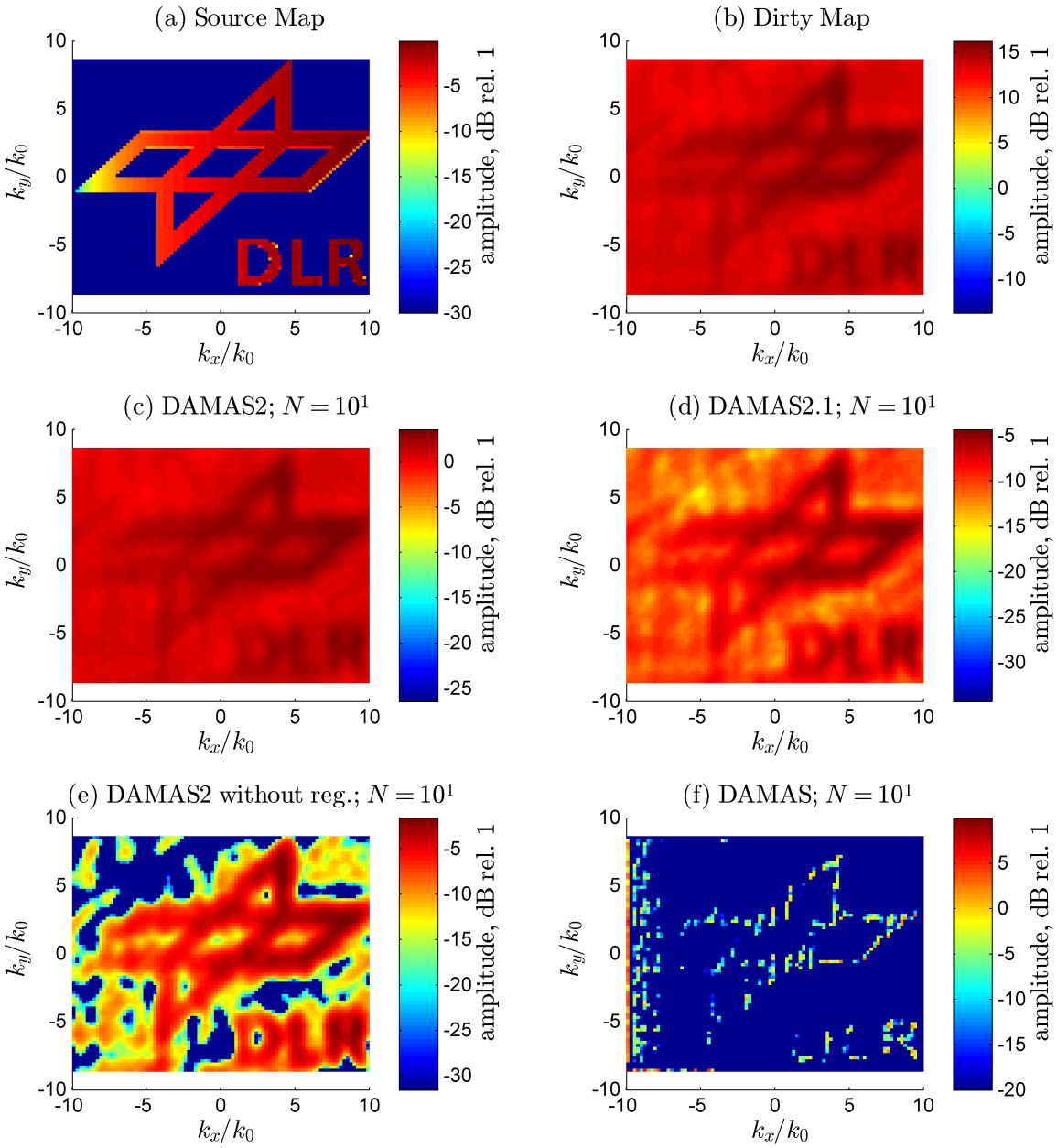

Figure 8: Results for a frequency of $f = 1000\,\mathrm{Hz}$ after $N = 10$ iterations
(a) source distribution of the synthetic test case
(b) dirty map
(c) result from DAMAS 2 with regularization filter
(d) result from DAMAS 2.1
(e) result from DAMAS 2 without regularization filter
(f) result from DAMAS

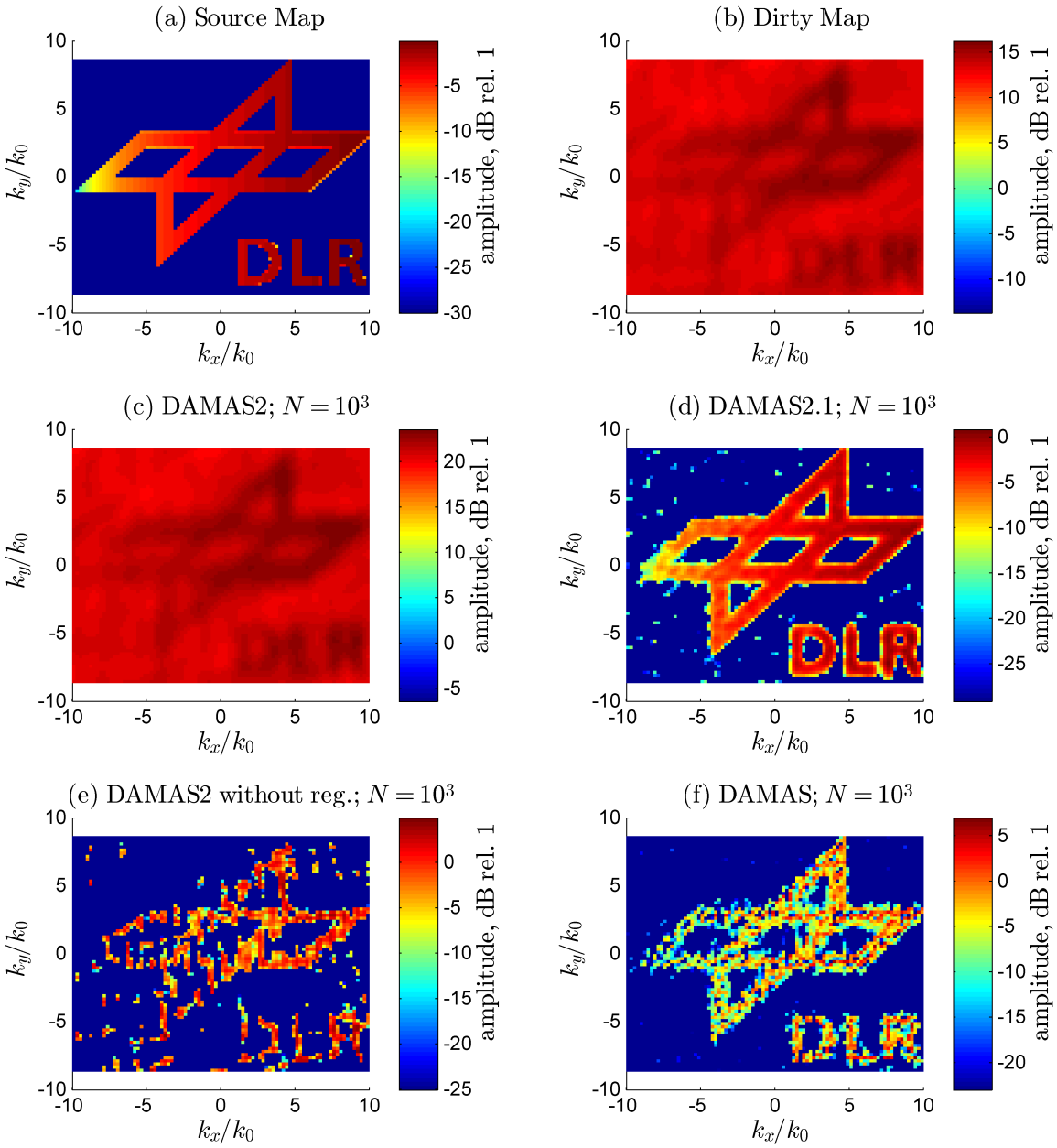

Figure 9: Results for a frequency of $f = 1000\,\mathrm{Hz}$ after $N = 1000$ iterations
(a) source distribution of the synthetic test case
(b) dirty map
(c) result from DAMAS 2 with regularization filter
(d) result from DAMAS 2.1
(e) result from DAMAS 2 without regularization filter
(f) result from DAMAS

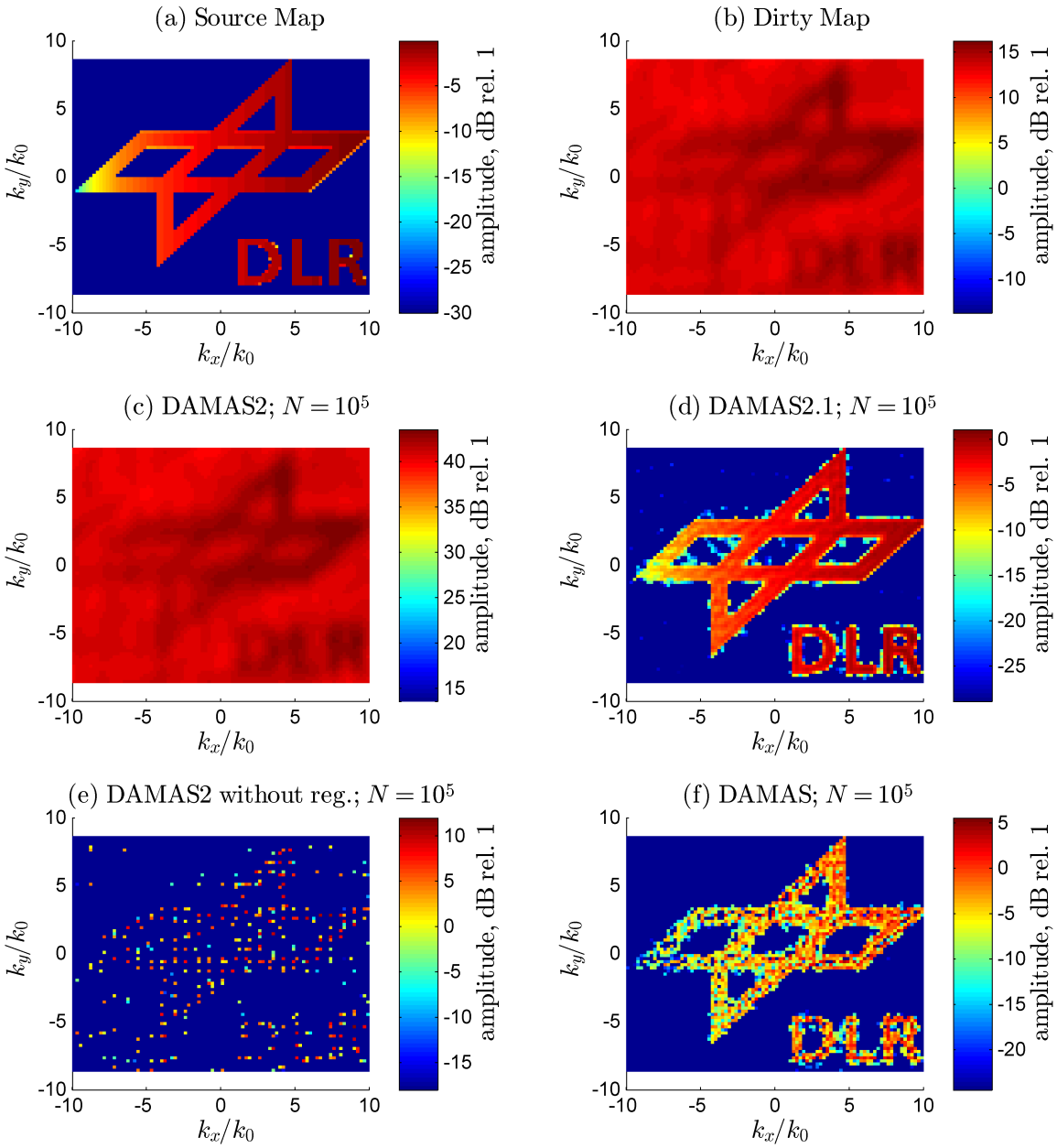

Figure 10: Results for a frequency of $f = 1000\,\mathrm{Hz}$ after $N = 100000$ iterations
(a) source distribution of the synthetic test case
(b) dirty map
(c) result from DAMAS 2 with regularization filter
(d) result from DAMAS 2.1
(e) result from DAMAS 2 without regularization filter
(f) result from DAMAS

noise level caused by the side lobes of all the distributed sources. Since - at a first approximation - the side lobe level is constant throughout the map, the dirty map has a very constant level as well with increments in the region where the source map exhibits high amplitudes. After $N = 10$ iterations, the DAMAS 2 algorithm was able to reduce the amplitude to approximately 3 dB, but did not yield any new detail. The DAMAS 2.1 algorithm reduced the amplitude as well and yields some new structure detail, but at the cost of contrast. The DAMAS 2 algorithm without regularization recovers a lot of detail at very reasonable amplitude and performs best after $N = 10$ iterations. The DAMAS algorithm again drastically reduces the background noise. However, after 10 iterations only parts of the underlying signet structure can be only assumed. The dominant part in the map is again a line of high amplitudes on the left hand side.

As shown in figure 12, after $N = 10^3$ iterations, the DAMAS 2 algorithm has become unstable. It appears that the dominant part of the *PSF* is located at high "frequencies" which are filtered out by the regularization. Therefore, the algorithm cannot reconstruct the dirty map. The DAMAS 2.1 algorithm was able to reconstruct the source map very well. Shape, amplitude and distributedness are all clearly visible. The result from the DAMAS 2 algorithm without regularization shows the basic signet shape and a reasonable amplitude. However it again appears as a accumulation of single spikes rather than a smooth surface. The DAMAS algorithm performs very well and recovers both the shape of the signet and its amplitude.

Increasing the number of iterations even further yields the results shown in figure 13. The DAMAS 2 algorithm has not recovered and still does not converge. The result from the DAMAS 2.1 algorithm shown in figure 13 (d) resembles a very good reconstruction of the underlying source map. It exhibits all the features of the original map. The same applies to the result from the DAMAS algorithm. The result from the DAMAS 2 algorithm without regularization has drifted towards a spike representation of the source map with increased amplitudes of the deconvolved map compared to the source map.

5.4 Residuals

The sum of differences between the dirty map and the source map convolved with the *PSF* are the residual of the algorithm. Each version of the DAMAS or DAMAS 2-algorithm uses the residual c to assess the quality of the source map determined. In the current case, the residual is normalized with the total number of grid points, M, in order to obtain the average deviation throughout the map, c^*.

$$c^* = \frac{1}{M} \sum_M (b - r) \tag{7}$$

The low-frequency case with $f = 100\,\text{Hz}$ is shown in figure 14. At a small number of iterations, the three variations of the DAMAS 2 algorithms start out equally well. The regular DAMAS 2 algorithm and the DAMAS 2 algorithm without regularization continuously rise by approximately 1.5 orders of magnitude as the number of iterations is increased to 10^5. The similar behavior can be explained by only low "frequency" content present in the *PSF* at this frequency. The residual from the DAMAS 2.1 algorithm drops slightly and appears to converge. The DAMAS algorithm starts at approximately 1 order of magnitude above the DAMAS 2 algorithms and is able to decrease the residual slightly. After $N = 10^5$ iterations, the differenc between the residual of the DAMAS 2.1 algorithm and the residual of the DAMAS algorithm has dropped to only 0.5 orders of magnitude.

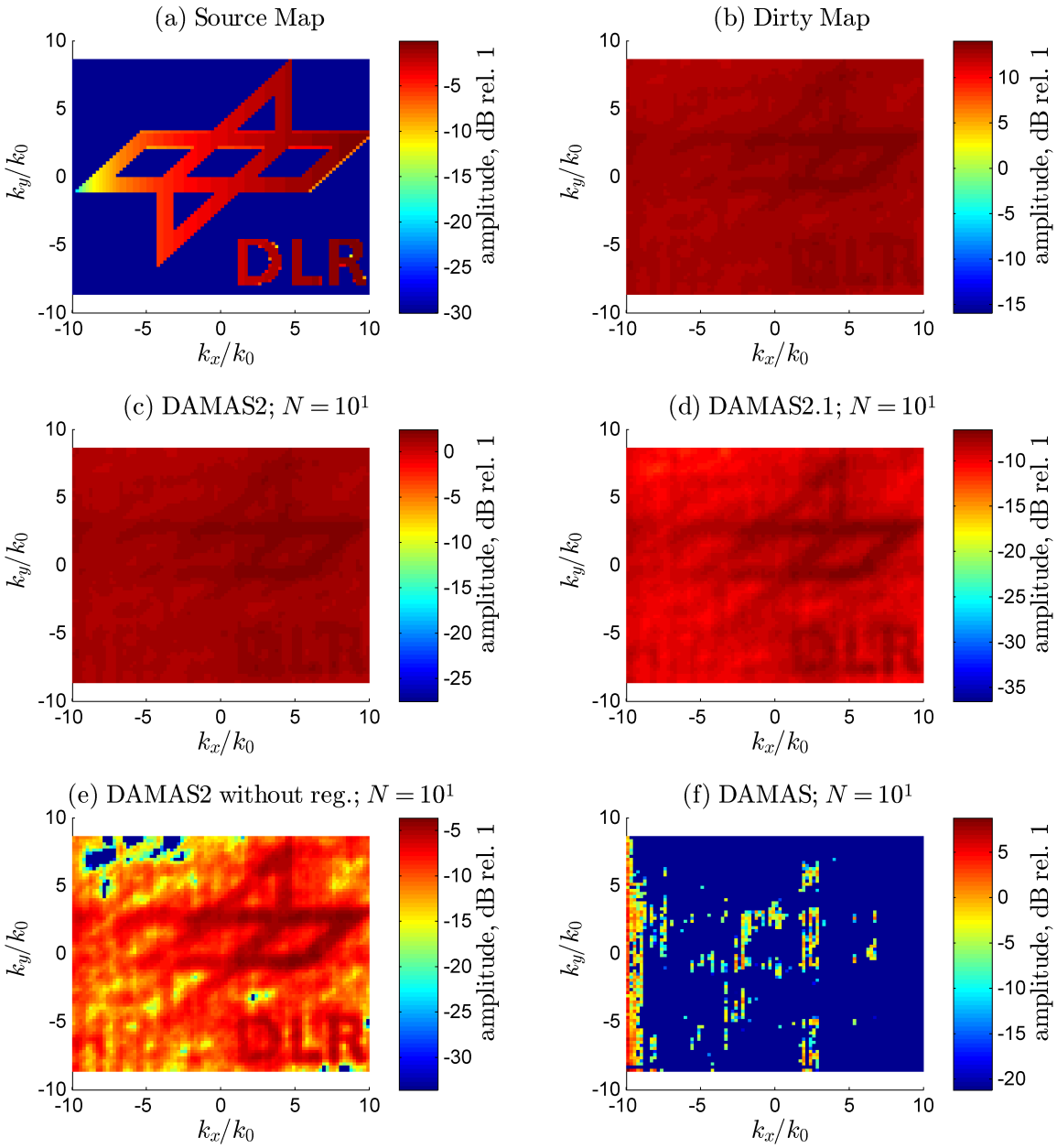

Figure 11: Results for a frequency of $f = 2500\,\mathrm{Hz}$ after $N = 10$ iterations
(a) source distribution of the synthetic test case
(b) dirty map
(c) result from DAMAS 2 with regularization filter
(d) result from DAMAS 2.1
(e) result from DAMAS 2 without regularization filter
(f) result from DAMAS

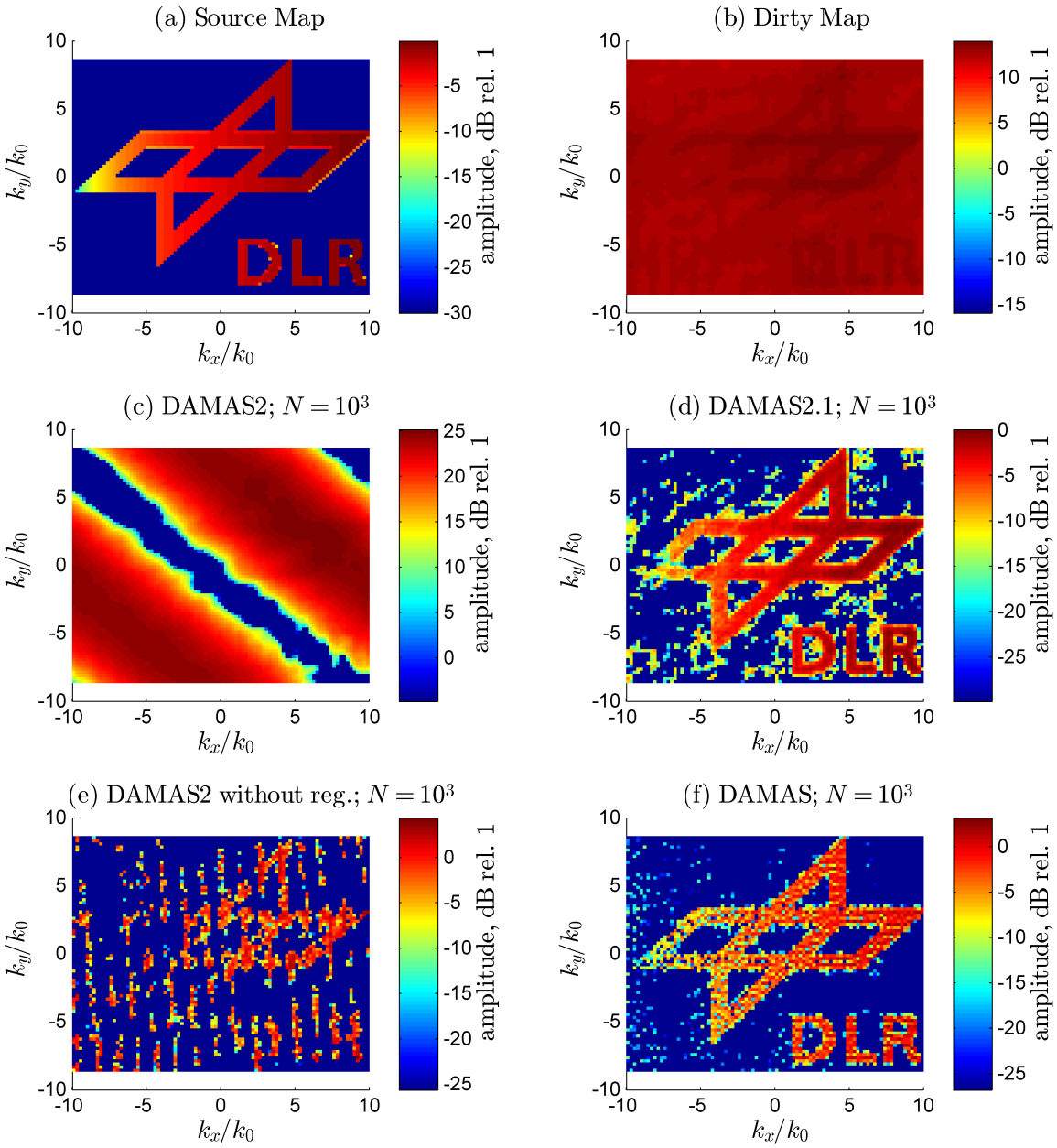

Figure 12: Results for a frequency of $f = 2500\,\mathrm{Hz}$ after $N = 1000$ iterations
(a) source distribution of the synthetic test case
(b) dirty map
(c) result from DAMAS 2 with regularization filter
(d) result from DAMAS 2.1
(e) result from DAMAS 2 without regularization filter
(f) result from DAMAS

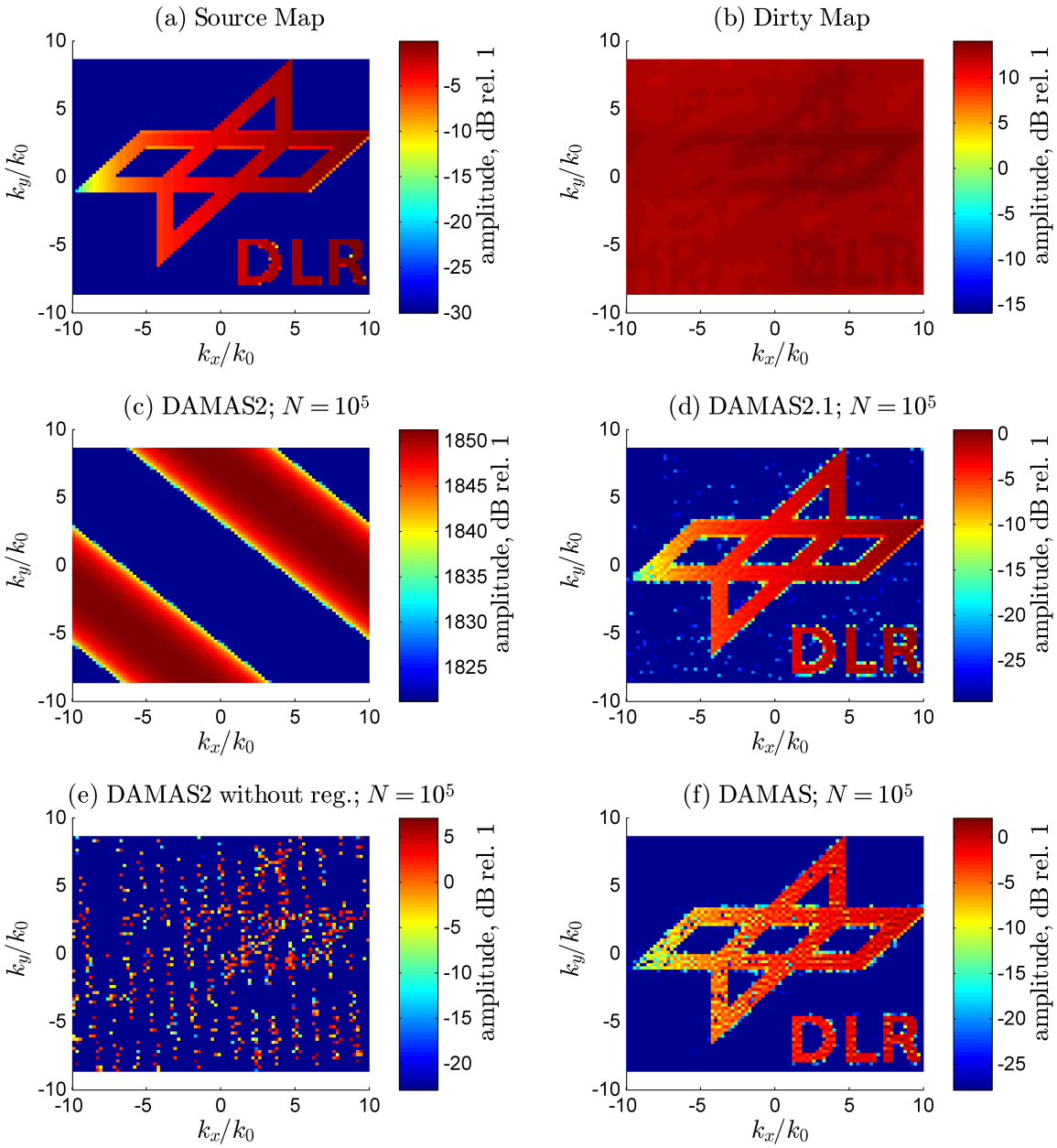

Figure 13: Results for a frequency of $f = 2500\,\mathrm{Hz}$ after $N = 100000$ iterations
(a) source distribution of the synthetic test case
(b) dirty map
(c) result from DAMAS 2 with regularization filter
(d) result from DAMAS 2.1
(e) result from DAMAS 2 without regularization filter
(f) result from DAMAS

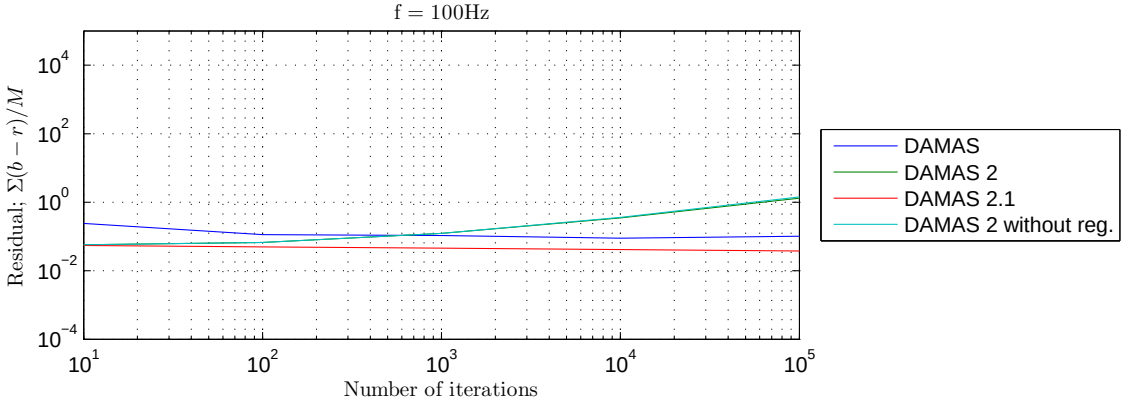

Figure 14: Residuals for different number of iterations for the test case at $f = 100\,\mathrm{Hz}$.

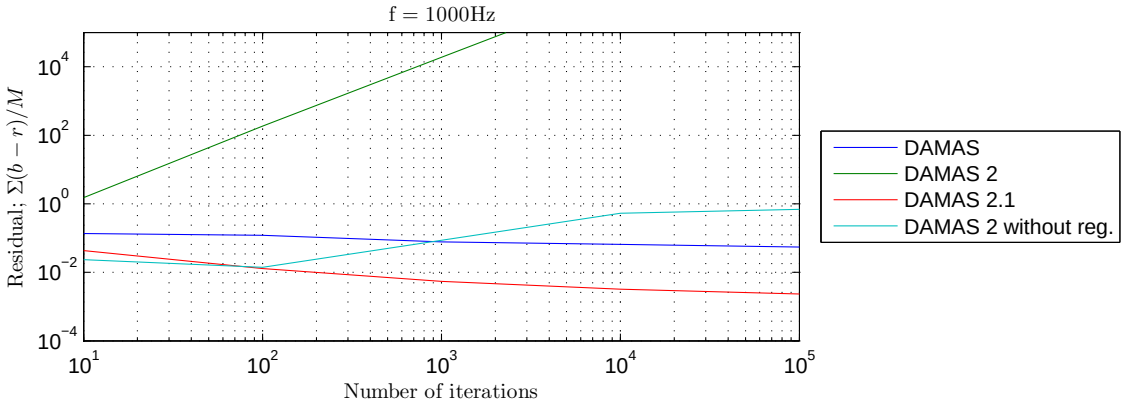

Figure 15: Residuals for different number of iterations for the test case at $f = 1000\,\mathrm{Hz}$.

At a medium frequency of $f = 1000\,\mathrm{Hz}$ - shown in figure 15 - both, the DAMAS and DAMAS 2.1 algorithm continuously reduce the residual. The DAMAS 2.1 algorithm has a lower residual throughout the number of iterations under consideration. The DAMS2 algorithm without regularization performs well at a low number of iterations, but then the resudal starts to rise between $N = 10^2$ and $N = 10^3$ iterations. The regular DAMAS 2 algorithm produces an unstable residual which rises constantly. It is supposed that at 100 iterations the DAMAS 2 algorithms using a small *PSF* start to produce spikes as result rather than distributed sources in order to compensate for the small *PSF* not being able to reconstruct the dirty map. The regular DAMAS 2 algorithm with its regularization filter set active seems to be especially affected by this.

Essentially the same phenomena as at $f = 1000\,\mathrm{Hz}$ occur at $f = 2500\,\mathrm{Hz}$, except that both, the DAMAS 2.1 and the DAMAS algorithm appear to have a better convergence than at $f = 1000\,\mathrm{Hz}$. This is shown in figure 16.

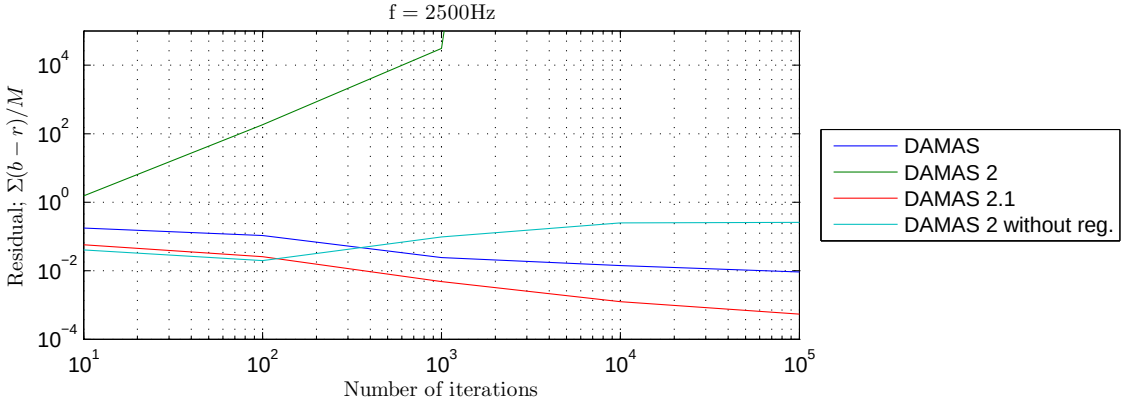

Figure 16: Residuals for different number of iterations for the test case at $f = 2500\,\mathrm{Hz}$.

6 TEST CASE 2: EXPERIMENTAL DATA

Experimental data was acquired in the Transonic Windtunnel Göttingen (TWG) underneath a high-subsonic turbulent boundary layer. The experimental setup consisted of a flat plate with elliptical nose, which had a sensor element included in its surface after a run length of 2.1 m. The sensing element contained 48 piezo-resistive pressure transducers of type ENTRAN EPE-S449-0.35B. The sensors were pinhole mounted, thus effectively reducing the sensitive surface from 2.4 mm to 0.5 mm - the bearing of the pinhole. The Helmholtz frequency of the pinhole mounting was estimated to be approximately 11 kHz. The reference-side of the pressure transducers lead into the plenum of the wind tunnel, which had a reduced ambient pressure of $p_0 = 50\,\mathrm{kPa}$. The wind tunnel was set to a speed of $M = 0.65$. The acceleration on the plate due to the thickening of the boundary layer lead to a speed of $M = 0.8$ present at the beginning of the sensing element in the plate. The static pressure at the beginning of the sensor element was measured to be $p_\infty = 32\,530\,\mathrm{Pa}$ which is the equivalent of a static pressure present at an altitude of approximately 30000 ft, or FL300. The acceleration of the flow lead to a drop in static temperature from a total temperature of $T_0 = 308\,\mathrm{K}$ present in the plenum lead to $T = 265.5\,\mathrm{K}$.

The evaluation is performed by applying a spatial Fourier transform on the cross-spectral elements of the pressure fluctuation data. The exact procedure is not important here. The analysis results in dirty maps with a shift-invariant point-spread function which makes it ideal for the application of DAMAS 2.

7 RESULTS FROM EXPERIMENTAL DATA

Results from the analysis of the experimental data set are presented for an iteration count of 2000 iterations. The three variations of DAMAS 2 presented here (DAMAS 2 with regularization, DAMAS 2 without regularization, and DAMAS 2.1) and three representative frequencies in close proximity of the frequencies used in the section evaluating the synthetical data are considered.

Results from evaluating the lowest frequency of $f = 117\,\mathrm{Hz}$ are shown in figure 17.

The dirty map of the wavenumber analysis for a frequency of 117 Hz is shown in figure 17

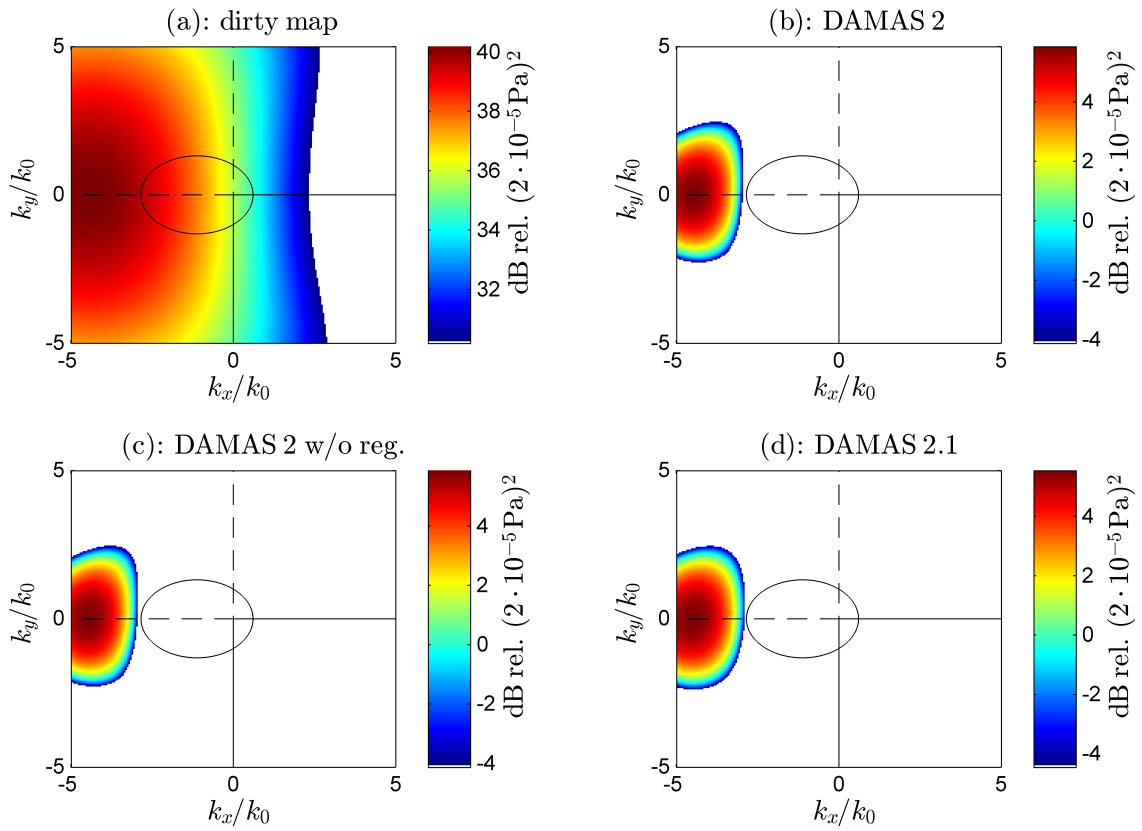

Figure 17: Results of the wavenumber analysis at $f = 117\,\text{Hz}$
(a) Dirty map
(b) Deconvolved map using DAMAS 2: 2000 iterations
(c) Deconvolved map using DAMAS 2 without regularization: 2000 iterations
(d) Deconvolved map using DAMAS 2.1: 2000 iterations

(a). A broad peak with an amplitude of approximately 39 dB is visible in the left side of the wavenumber spectrum at $k_x/k_0 \approx -4.5$ and $k_y/k_0 = 0$. The position of this peak is outside the acoustic region. The peak being outside the acoustic region usually means that the propagation velocity of the pressure fluctuations is lower than the speed of sound and therefore must be flow-related. Considering that the peak position is located at negative k_x-value this would mean that a strong back-flow was present in the measurement. The peak position does not exhibit the characteristic shape of a convective ridge resulting from different distances in flow and cross-flow direction over which a coherent signal is produced by the turbulent structures over the measurement area. The findings at the evaluation frequency rather point towards an erroneous display of the acoustic region which is dependent on the Mach number of the flow. In the experiment, the incident flow was set to a Mach number of $M = 0.65$. Due to the acceleration caused by the blocking of the wind tunnel and the thickening of the boundary layer, the local Mach number was raised to approximately $M = 0.8$ which would expand the acoustical region further towards negative values of k_x.

All three variations of the DAMAS 2-algorithm perform reasonably well when applied to the

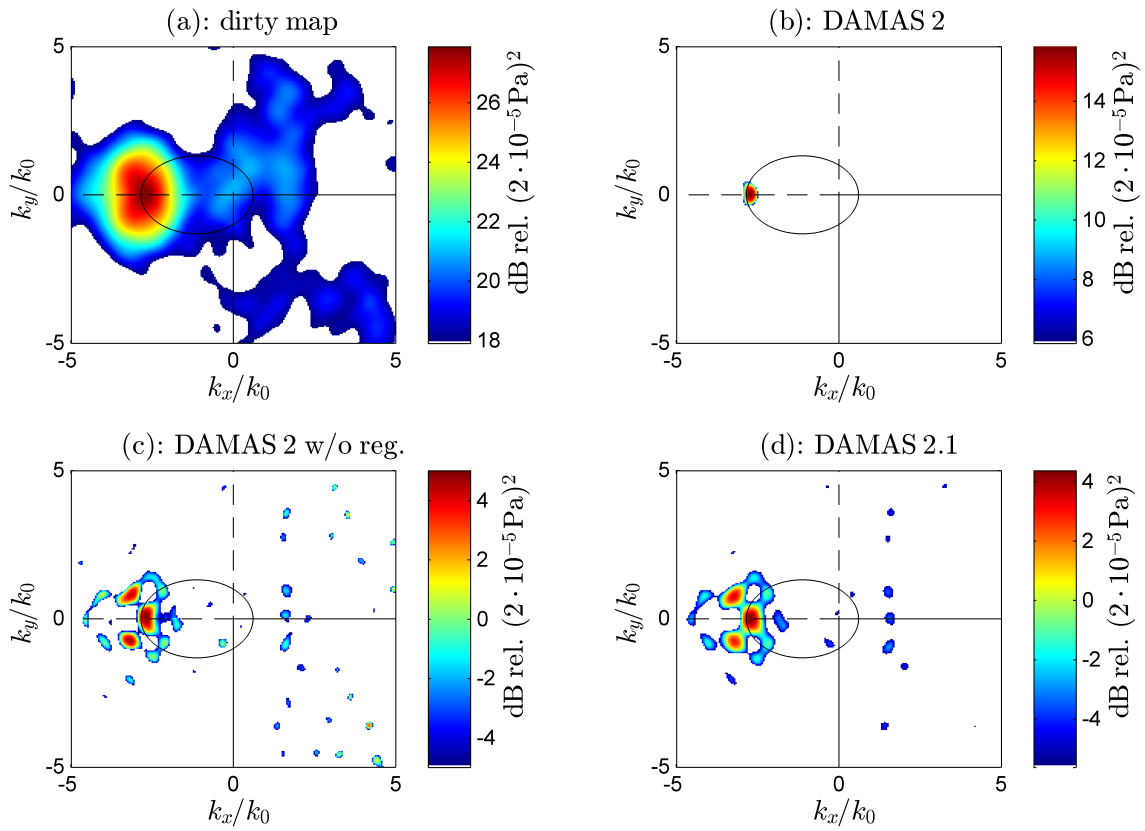

Figure 18: Results of the wavenumber analysis at $f = 937\,\text{Hz}$
(a) Dirty map
(b) Deconvolved map using DAMAS 2: 2000 iterations
(c) Deconvolved map using DAMAS 2 without regularization: 2000 iterations
(d) Deconvolved map using DAMAS 2.1: 2000 iterations

dirty map. The resulting maps are very similar: The amplitude is reduced drastically from 39 dB to approximately 6 dB. The extent of the peak is reduced considerably as shown in figures 17 (b)-(d). The fact that the amplitude of the peak is reduced to a large extent by the deconvolution procedure indicates that the pressure fluctuation propagating over the array is not a distinct point source but rather a diffuse distributed source.

Results from the wavenumber evaluation at a frequency of $f = 937\,\text{Hz}$ are shown in figure 18. Again, the dirty map is shown in part (a) of that figure. A peak is visible on the rim of the acoustic domain at $k_x/k_0 \approx -2.5$ and $k_y/k_0 = 0$. The peak has an amplitude of approximately 28 dB. The position on the rim of the acoustic domain indicates that the cause for this particular pressure fluctuation is of acoustic nature. On the right-hand side of the spectrum a slightly elevated part appears where the convective ridge is assumed to be at $k_x/k_0 \approx +1.7$. Whether or not this can be considered a valid signal or is just an artifact of either noise or the point-spread function of the peak is uncertain.

Using the regular DAMAS 2 algorithm with regularization filter results in a reduction of the peak to a single dot after $N = 2000$ iterations. The deconvolved map gives the impression that

a peak of amplitude 15 dB is the only source present at this frequency. Its position on the rim of the acoustic region indicates that a single acoustic wave is present over the array, propagating upstream precisely parallel to the array surface.

The indications change when using either the DAMAS 2 algorithm without the regularization filter or the DAMAS 2.1 algorithm for deconvolution. Three distinct sources of pressure fluctuations propagating upstream are visible in both, figure 18 (c) and (d). The dominant peak is still located at the same position as in the dirty map and in the deconvolution with the regular DAMAS 2 with regularization filter. Two adjacent sources have however appeared slightly further away from the origin and at a symmetrical offset about the k_x-axis. This sheds a new light on the interpretation, as the two re-emerged sources are probably of acoustic nature as well and the Mach number for the setup of the acoustic region is chosen too small once again. The intersection of an ellipse piercing the two newly-found sources with the k_x-axis is estimated to be at approximately $k_x/k_0 = -4$. This indicates a frequency-dependent drop in the local Mach number to be used for the distortion of the acoustic region towards higher frequencies. Using the new interpretation of local Mach number, the dominant peak found initially is still representative of a pressure fluctuation propagating at the speed of sound in upstream direction, but now it appears not to be parallel to the surface any more. It rather appears to have an incident angle over the array which could be linked to an acoustic wave propagating diagonally upstream and being reflected from the upper and lower wind tunnel walls. The amplitude of the dominant pressure fluctuation is found to be lowered to approximately 4.5 dB when using the regular DAMAS 2 algorithm without regularization and to approximately 4 dB using the DAMAS 2.1 algorithm. The re-emerged sources are approximately 2 dB below the dominant source in each case.

On the right-hand side of the wavenumber spectrum no hint of a convective ridge is visible when using the regular DAMAS 2 algorithm with regularization filter shown in figure 18 (b). When discarding the regularization filter, several peaks of low amplitude become visible in the area where the convective ridge is expected ($k_x/k_0 \approx 1.7$). However, the lack of the filter also introduces many other peaks which make an interpretation of the findings difficult. When using the DAMAS 2.1 algorithm, only the peaks in the region where the convective ridge is expected are visible and no other peaks are introduced. Supposedly the convective ridge becomes visible here, which is a very valuable information in the source map.

A dirty map at the third frequency of $f = 2490$ Hz is shown in figure 19 (a). A dominant convective ridge is visible at a center point of $k_x/k_0 \approx 1.7$ and $k_y/k_0 = 0$ outside the acoustic domain. The extend of the convective ridge is considerably larger in k_y-direction than it is in k_x-direction resulting from a larger distance in x-direction over which the pressure fluctuations underneath the turbulent boundary layer are producing a coherent signal on the measurement surface. Both, the position in the wavenumber spectrum and the characteristic shape strongly suggest that this in fact is a convective ridge caused by the convection of turbulent structures in the flow. The amplitude of the convective ridge is slightly above 18 dB and considerable background noise is present approximately 6 dB below the peak value.

When using the regular DAMAS 2 algorithm with regularization filter for deconvolution, the convective ridge is still visible and exhibits its characteristic features as shown in figure 19 (b). The algorithm reduces the maximum amplitude of the convective ridge from slightly above 18 dB to a level of approximately 17.5 dB. When discarding the regularization filter the shape of the convective ridge is altered from its rhombic shape towards a rather spiky appearance

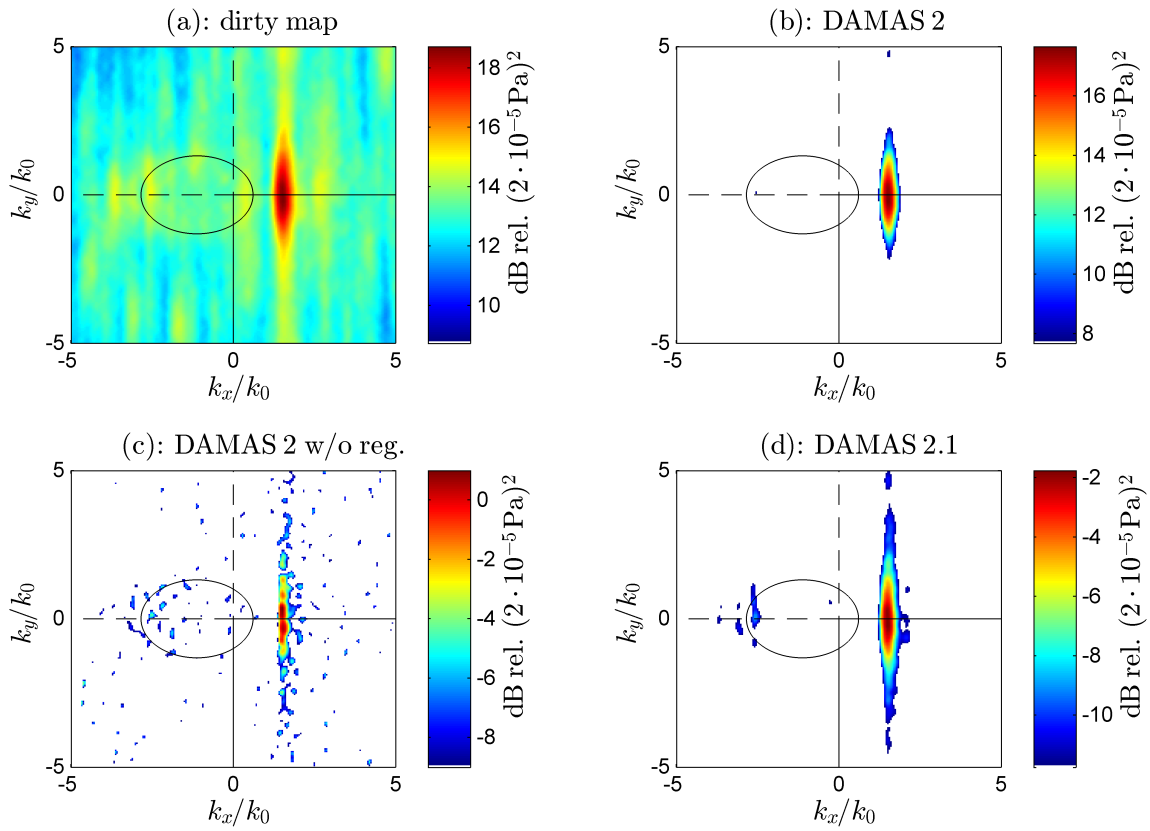

Figure 19: Results of the wavenumber analysis at $f = 2490\,\mathrm{Hz}$
(a) Dirty map
(b) Deconvolved map using DAMAS 2: 2000 iterations
(c) Deconvolved map using DAMAS 2 without regularization: 2000 iterations
(d) Deconvolved map using DAMAS 2.1: 2000 iterations

with a maximum amplitude of 0.5 dB. Also, a considerable amount of peaks are introduced in the acoustic region and at wavenumbers beyond the convective ridge. The peaks beyond the convective ridge are most probably non-physical artifacts: Due to their position they would be assigned to a convective flow-phenomenon. Their shape however does not denote such a propagation mechanism since a single peak indicates a uniform loss of coherence in all direction. Any source related to a flow-phenomenon would most likely exhibit a larger extent of coherence in flow direction. Due to this discrepancy the peaks are considered to be artifacts of the deconvolution algorithm. Whether or not the peaks inside the acoustic region are artifacts or actually present on the surface cannot be determined or analyzed: acoustic propagation allows for the presence of peaks.

When using the DAMAS 2.1 algorithm - shown in figure 19 (d), the peaks are not present any more in both the acoustic region and beyond the convective ridge. Also, the shape of the convective ridge has returned to its original rhombic shape and its amplitude has been reduced to approximately $-2\,\mathrm{dB}$. A slight peak with an amplitude of $-8\,\mathrm{dB}$ on the opposite side of the convective ridge at approximately $k_x/k_0 = -2.5$ indicates an acoustic wave still present at this

frequency propagating upstream.

8 CONCLUSION

The choice of a deconvolution algorithm can have a large influence on the result. Compared to the DAMAS 2 algorithm and its variation without regularization filter, the proposed DAMAS 2.1 algorithm performs significantly better at deconvolution on synthetic data. It is able to reconstruct most of the underlying source maps used in this investigations without the necessity of a regularization filter.

At high frequencies the DAMAS 2.1 performs equally well as the original DAMAS algorithm in terms of "looks" of the source map and even better than the DAMAS algorithm when looking at the residuals. At low frequencis, all algorithms under consideration are not able to cope with the large main lobe width of the *PSF*. In terms of execution speed, the DAMAS 2.1 algorithm outperforms the DAMAS algorithm by approximately 3 orders of magnitude: one drawback of the DAMAS algorithm is the rather slow convergence, which is most likely to result from the Gauss-Seidel iteration method. The DAMAS 2-algorithms have implemented a Richardson method which appears to converge faster.

The regular DAMAS 2 appears to become unstable at higher frequencies and a large number of iterations. The reason for this is the low-pass filtering of the regularization method which does not allow reconstruction of the dirty map with a detailed *PSF*. When loosing the filter, the instability vanishes but the source maps suffer from the high-frequency noise mentioned in the original DAMAS 2 paper. As shown in the present paper, this noise results from an insufficient size of the *PSF* which cannot be used for the reconstruction of the dirty map. Expanding the point-spread function leads to a better and - as shown with synthetic data - more reliable result at only a moderate increase of computational effort. Its usage is therefore strongly recommended when using the DAMAS 2.1 algorithm for deconvolution, especially when distributed sources are present.

When applying the algorithms to experimental data, the regular DAMAS 2 with regularization does not give detailed insight into the source structures present in the map. This may lead to a misinterpretation of the dataset as has been shown. The reason for this lies in the regularization which acts as a low-pass filter and prohibits the forming of fragile and detailed source structures during the iteration process.

It should be kept in mind that the algorithm proposed is considered for the use of shift-invariant point spread functions. An application to non-shift invariant problems is considered to be not applicable due to the large dimensions of the point-spread function required for the algorithm. If it were used for such problems, an application at low frequencies should be seeked, where the influence of shift-variance is considered less than at higher frequencies.

REFERENCES

[1] C. Bahr and L. Cattafesta. "Wavespace-based coherent deconvolution." In *18th AIAA/CEAS Aeroacoustics Conference*. American Institute of Aeronautics and Astronautics, 2012. URL http://dx.doi.org/10.2514/6.2012-2227.

[2] T. F. Brooks and W. M. Humphreys. "A deconvolution approach for the mapping of acoustic sources (damas) determined from phased microphone arrays." *Journal of Sound and Vibration*, 294(4–5), 856 – 879, 2006. ISSN 0022-460X. doi:http://dx.doi.org/10.1016/j.jsv.2005.12.046. URL http://www.sciencedirect.com/science/article/pii/S0022460X06000289.

[3] R. Dougherty. "Extensions of damas and benefits and limitations of deconvolution in beamforming." In *11th AIAA/CEAS Aeroacoustics Conference*. American Institute of Aeronautics and Astronautics, 2005. URL http://dx.doi.org/10.2514/6.2005-2961.

[4] K. Ehrenfried and L. Koop. "A comparison of iterative deconvolution algorithms for the mapping of acoustic sources." *AIAA Jounal*, 45(7), 1584–1595, 2006. URL http://dx.doi.org/10.2514/1.26320.

[5] S. Haxter and C. Spehr. "Infinite beamforming: Wavenumber decomposition of surface pressure fluctuations." pages 2014–05, 2014. URL http://www.bebec.eu/Downloads/BeBeC2014/Papers/BeBeC-2014-04.pdf.

[6] S. Haxter, C. Spehr, M. Hartmann, J. Ocker, H. Tokuno, and G. Wickern. "Improving the performance of aeroacoustic measurements beneath a turbulent boundary layer in a wake flow." In *AIAA Aviation*. American Institute of Aeronautics and Astronautics, 2014. URL http://dx.doi.org/10.2514/6.2014-3289.

[7] E. Sarradj. "Three-dimensional acoustic source mapping." In *Proceedings on CD of the 4th Berlin Beamforming Conference*, pages 2012–11. 2012. URL http://www.bebec.eu/Downloads/BeBeC2012/Papers/BeBeC-2012-11.pdf.